Electronic Supplementary Material (ESI) for Journal of Materials Chemistry A.

Supporting information (Investigation of Sodium Insertion in Hard Carbon with Operando Small Angle Neutron Scattering)

Hard carbon SAXS characterisation

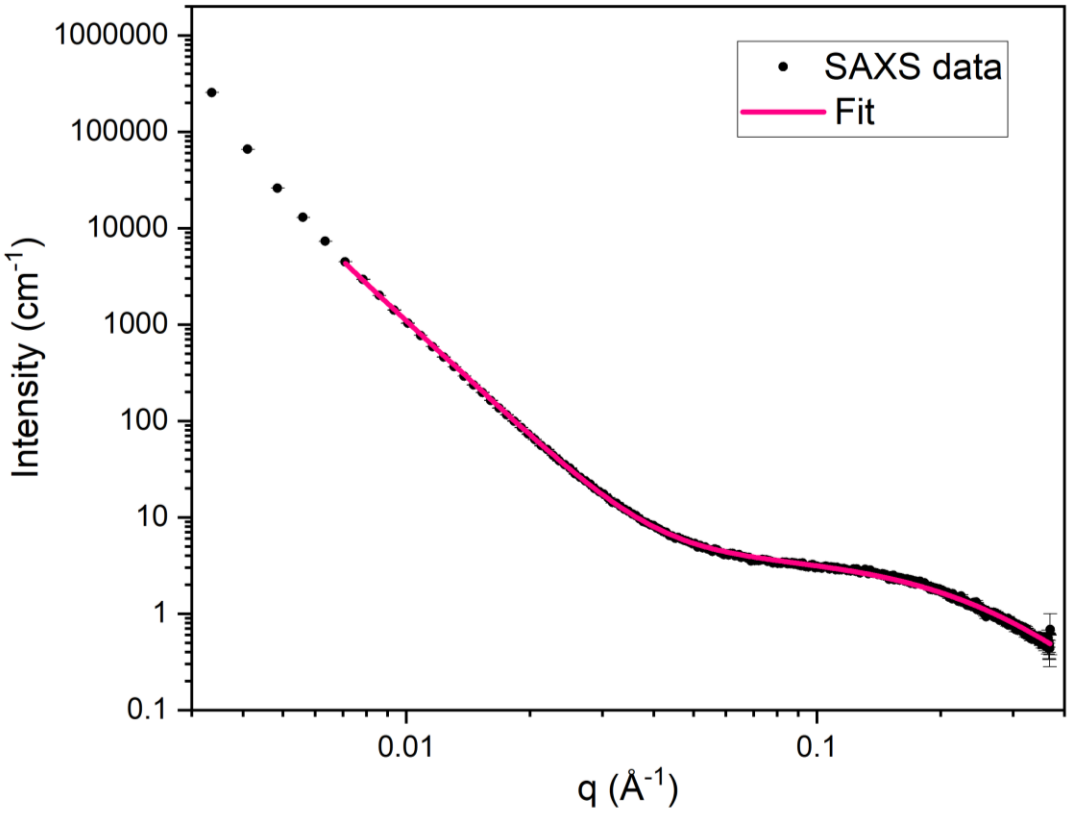

S1. SAXS data (black) and fit (pink) of commercial hard carbon.

The SAXS data have been fit using the model described in Ref S1:

$$I(Q) = \frac{A}{Q^4} + \frac{Ba_0^3}{(1 + a_0^2 Q^2)^2} + D$$

Where A, B are scale factors, D is a background term, and a_0 is the correlation length. The pore size can be estimated from the correlation length a_0

$$R = a_0 \times \sqrt{10}$$

Where R is the pore radius in angstrom. For this data, the correlation length was obtained a_0 = 3.66, to give a pore size of R = 11.6 Å.

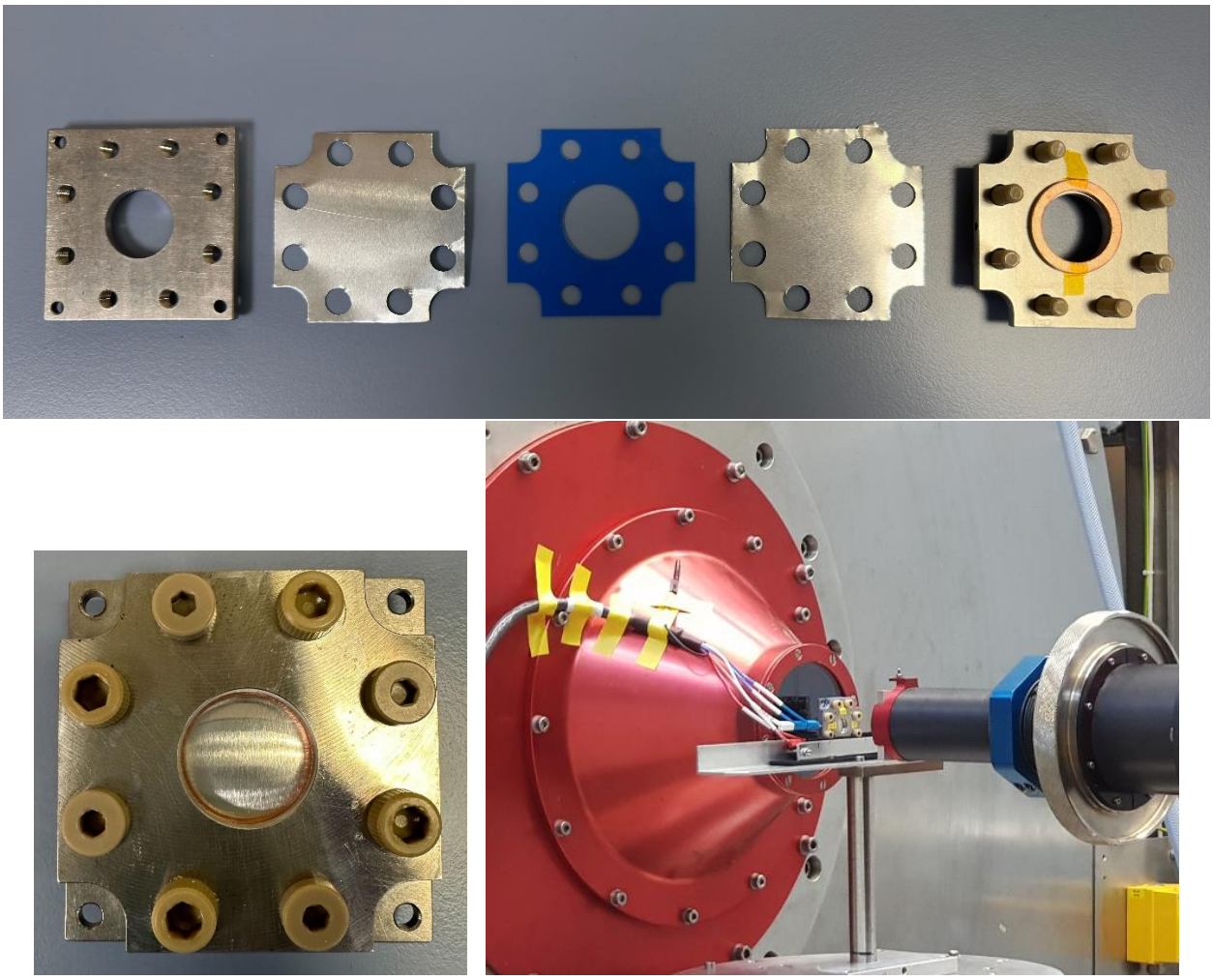

S2. (Upper) Left to right: front stainless steel casing, Al window/current collector, fluorosilicate gasket, Al window/current collector, back stainless steel casing with copper washer and PEEK screws. (Lower left) Assembled operando cell. (Lower right) Operando cell on the SANS-I beamline at PSI.

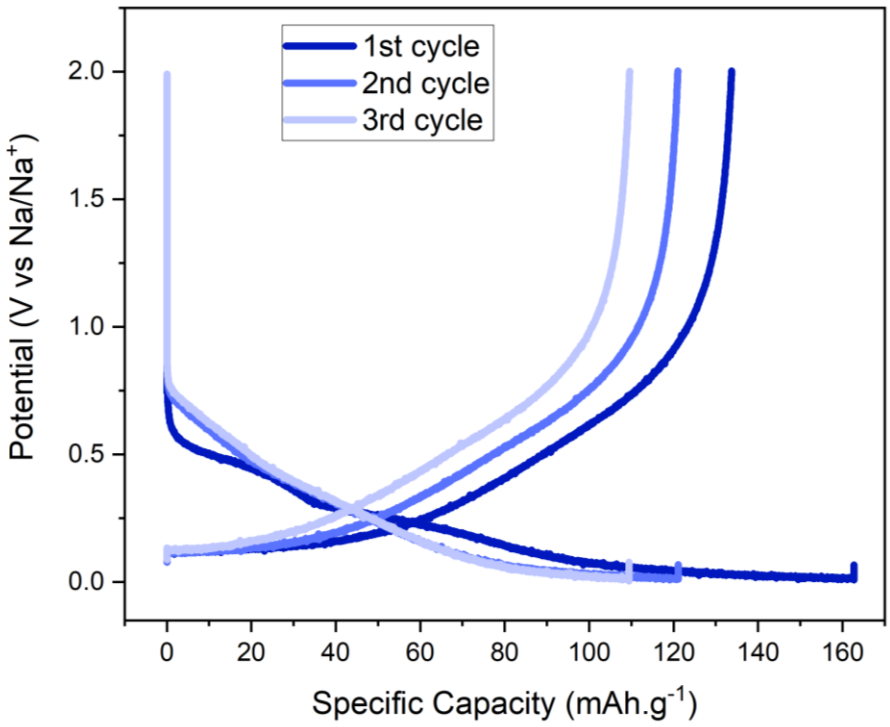

S3. Offline electrochemical cycling of the cell showing 3 cycles, with an initial coulombic efficiency of 82%. N.B The copper washer, which is used to increase pressure within the cell and improve the seal, was not used for these tests resulting. This is the likely cause for the lower capacities compared to those achieved during the operando experiment (197 mAh.g^{-1}).

Operando analysis

Batch fitting was carried out in SASview using the model described in Equation 1 on the Q-range 0.021-0.42 Å^{-1}. Some parameters were held constant as they either should not vary or are highly correlated to other parameters. The Porod constant (p) was held at 4, the overall scale factor was held at 0.00000047146. The C_1 and C_2 parameters are both related to the pore-pore spacing (d) and correlation length (ξ), and as expected these are highly correlated. Allowing both to refine produced an unstable fit so we chose to fix one (C_1 = 10.55) and allow the other to vary (C_2) but don't attempt to interpret the change in d and ξ. The other parameters – background B, I_p and I_{np} are also refined. Below are selected fitted SANS patterns, and the table outlines the potential, fit (X^2), and refined parameters of these fits.

From the parameters obtained from the fitting, the SLD contrast can be extracted using the following equations:

$$\Delta SLD^2 = \frac{I_{np}\rho_{struc}}{8\pi\phi\xi^3}\left(1+\left(\frac{2\pi\xi}{d}\right)^2\right)^2 \qquad \textbf{(Equation S1)}$$

$$d = 2\pi\left[\frac{1}{2}C_2^{-\frac{1}{2}} - \frac{C_1}{4C_2}\right]^{-\frac{1}{2}}$$

$$\xi = 2\pi\left[\frac{1}{2}C_2^{-\frac{1}{2}} + \frac{C_1}{4C_2}\right]^{-\frac{1}{2}}$$

Where d is the pore-pore distance, ξ is the correlation length of the extension of order, ϕ is the pore volume fraction (0.33), and ρ_{struc} is the density. The first equation is rearranged from Eq 9. in Ref S2 to give the SLD contrast

$$I_{np} = \frac{8\pi}{\rho_{struc}}\phi(\Delta SLD)^2\frac{\xi^3}{\left(1+\left(\frac{2\pi\xi}{d}\right)^2\right)^2}$$

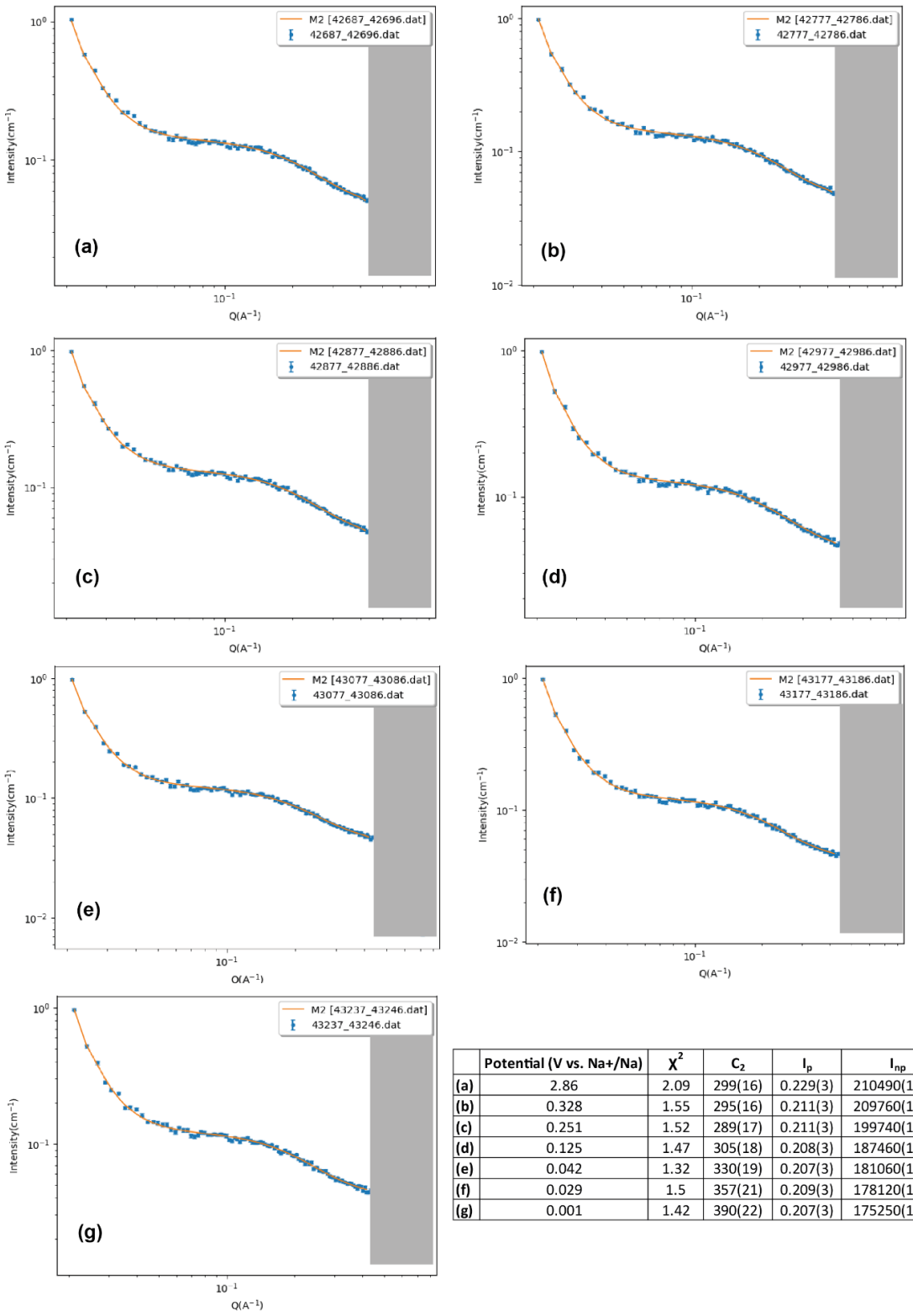

	Potential (V vs. Na+/Na)	χ^2	C_2	I_p	I_{np}
(a)	2.86	2.09	299(16)	0.229(3)	210490(1631)
(b)	0.328	1.55	295(16)	0.211(3)	209760(1638)
(c)	0.251	1.52	289(17)	0.211(3)	199740(1649)
(d)	0.125	1.47	305(18)	0.208(3)	187460(1616)
(e)	0.042	1.32	330(19)	0.207(3)	181060(1573)
(f)	0.029	1.5	357(21)	0.209(3)	178120(1541)
(g)	0.001	1.42	390(22)	0.207(3)	175250(1513)

S4. Fitting (orange) of selected SANS data (blue) and table showing refined parameters and goodness of fit. Note the χ^2 is the reduced parameter that has been normalised to the number of degrees of freedom.

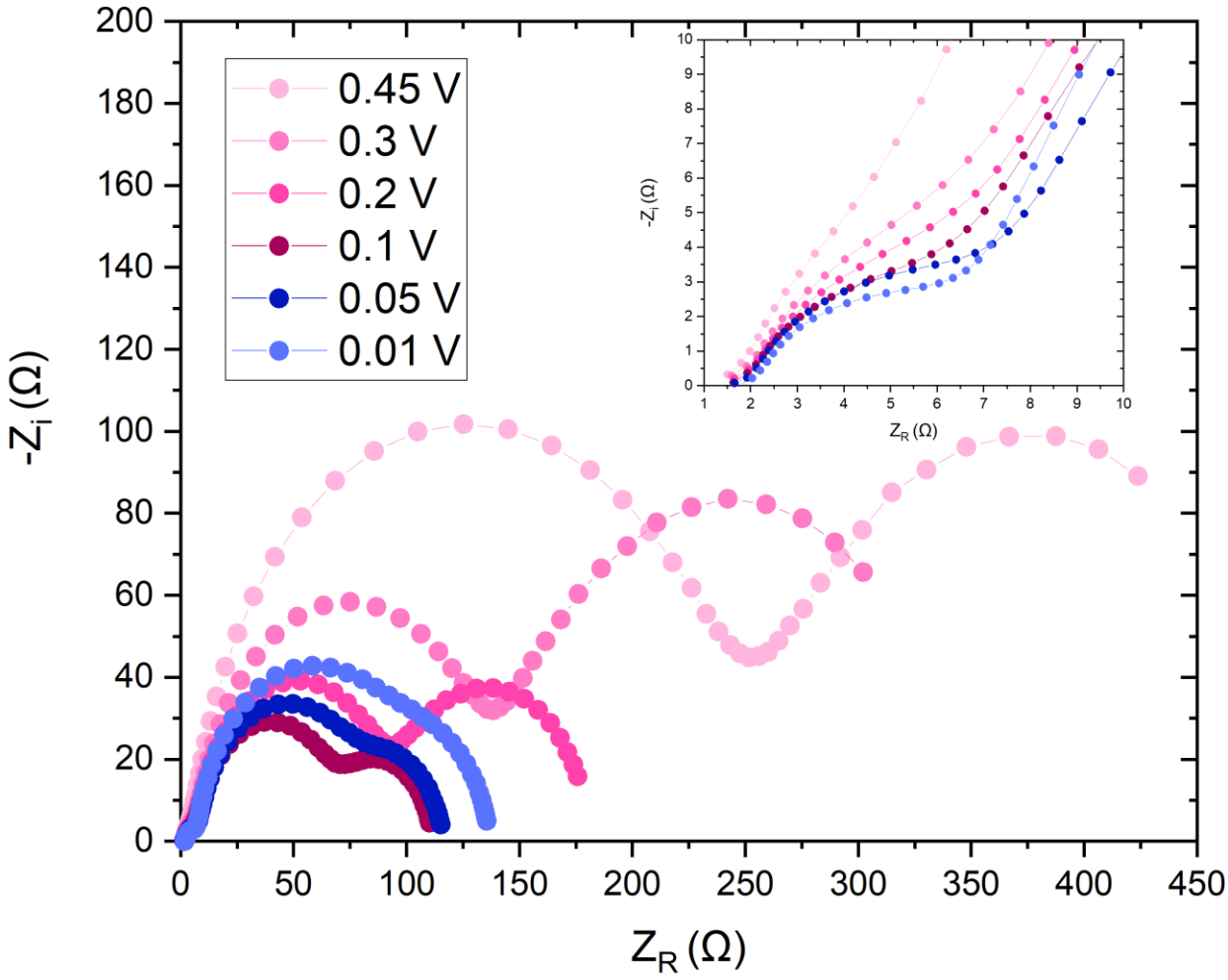

S5. Nyquist plots obtained from electrochemical impedance measurements of the cell at various points during discharge. The frequency range used as from 1 Hz to 1 MHz at an amplitude of 10 mV collecting 10 points per decade in logarithmic spacing. The 3 highest frequency points were omitted due to low accuracy.

SLD calculations

Initially, the ΔSLD is the difference in SLD between the carbon and the pores. The SLD of the carbon is calculated using a density of 2, which is slightly below that of graphite (2.2). The carbon is described as graphite-like regions, and from XRD studies we know that the interlayer spacing in HC is larger than that of graphite, therefore it is reasonable that the density is slightly lower. This estimation has been made elsewhere.[S3] As we have performed a background subtraction using a cell containing the same amount of electrolyte, we assume the SLD of the pores is zero. This also covers the unknown of pore-filling, as we don't have the means to see if the pores are filled with electrolyte, partially filled, or not filled at all. This won't impact our results as we are only trying to interpret the relative change.

In order to estimate the changes in ΔSLD^2 during the intercalation and pore filling processes we need to estimate the composition and density changes with sodiation of the carbon and pores, and these are referred to as sodiated carbon and sodiated electrolyte when additional sodium has been introduced electrochemically. Obtaining the Na content from the electrochemistry will provide the composition and mass change. The number of moles of sodium ions, assuming the capacity is assigned to a single process, will be related to the current applied over the time of the relevant region:

$$n_{Na} = \frac{t \times I \times e}{6.022 \times 10^{-23}}$$

Where *t* is the time in seconds, I is the current in Amps (0.000275 A), and e is the number of electrons in 1 Coulomb of charge. The composition of the sodiated carbon or sodiated electrolyte in the closed pores is calculated from this, as is the mass change. For intercalation the final composition of the sodiated carbon calculated from the electrochemistry from the second region is NaC_{25} which is consistent with reported values also derived from electrochemistry,[S4,S5] and the composition found in the corresponding region in a molecular dynamics study.[S6]

The volume change is also required to obtain the density change, and we estimate this using a recent dilatometry study.[S7] The experiment measures thickness change of the hard carbon with sodiation in operando. We justify this as an estimate for our system as they use the same binder and electrolyte, the capacity they achieve (170 $mAh.g^{-1}$) is comparable to ours, as is the relative capacity resulting from the sloping and plateau regions. For the sloping region we estimate a volume change of 9.27%, and for the plateau region a change of 4.6%. We linearly extrapolate these changes over the respective regions.

The ΔSLD is calculated taking into account the volume ratio of carbon:pores of 2:1

$$\Delta SLD = SLD_{carbon} - 0.5 \cdot SLD_{pores}$$

	Density (g/cm^3)	**SLD ($10^{-6}/Å^2$)**
Hard carbon	1.48	4.934
Graphite (in HC)	2	6.667
$NaPF_6$ in EC/DEC	1.26	1.531
NaC_{25}*	1.97	6.236
$Na_{14}PF_6$ in EC/DEC **	1.50	1.741

Table 1. Table showing the densities and calculated SLDs of the pristine carbon and electrolyte, as well as the sodiated versions of these (NaC25 and Na14PF6, respectively).

** Density of Sodiation graphite NaC25 slightly lower than HC graphite as the volume change (9.27% from dilatometry study) is larger than the mass change.*

*** Density of sodiated electrolyte calculated using volume increase of 4.6% (from dilatometry measurements).*

References

[S1] Au, H. Et al. A revised mechanistic model for sodium insertion in hard carbons *Energy Environmental Science* **13**, 3469-3479 (2020).

[S2] Saurel, D. et al. A SAXS outlook on disordered carbonaceous materials for electrochemical energy storage *Energy Storage Materials* **21**, 162-173 (2019).

[S3] Bridges, C.A., Sun, X.G., Zhao, J., Parans Paranthaman, M. & Dai, S. In Situ Observation of Solid Electrolyte Interphase Formation in Ordered Mesoporous Hard Carbon by Small-Angle Neutron Scattering *The Journal of Physical Chemistry C* **14**, 7701-7711 (2012).

[S4] Deringer, V.L. et al. Towards an atomistic understanding of disordered carbon electrode materials *Chem. Comm.* **47** (2018).

[S5] Stratford, J.M. et al. Correlating Local Structure and Sodium Storage in Hard Carbon Anodes: Insights from Pair Distribution Function Analysis and Solid-State NMR *J. Am. Chem. Soc.* **35**, 14274-14286 (2021).

[S6] Li, J., Peng, C., Li, J., Wang, J. & Zhang, H. Insight into Sodium Storage Behaviors in Hard Carbon by ReaxFF Molecular Dynamics Simulation *Energy & Fuels* **36**, 5937-5952 (2022).

[S7] Alptekin, H. et al. Sodium Storage Mechanism Investigations through Structural Changes in Hard Carbons *ACS Applied Energy Materials* **3**, 9918-9927 (2020).